

A combined thermodynamics and first principles study of the electronic, lattice and magnetic contributions to the magnetocaloric effect in  $\text{La}_{0.75}\text{Ca}_{0.25}\text{MnO}_3$

This content has been downloaded from IOPscience. Please scroll down to see the full text.

2016 J. Phys. D: Appl. Phys. 49 285001

(<http://iopscience.iop.org/0022-3727/49/28/285001>)

View [the table of contents for this issue](#), or go to the [journal homepage](#) for more

Download details:

IP Address: 129.174.21.5

This content was downloaded on 21/06/2016 at 16:11

Please note that [terms and conditions apply](#).

# A combined thermodynamics and first principles study of the electronic, lattice and magnetic contributions to the magnetocaloric effect in $\text{La}_{0.75}\text{Ca}_{0.25}\text{MnO}_3$

R K Korotana<sup>1</sup>, G Mallia<sup>1</sup>, N M Fortunato<sup>2</sup>, J S Amaral<sup>2,3</sup>, Z Gercsi<sup>4</sup>  
and N M Harrison<sup>1</sup>

<sup>1</sup> Department of Chemistry, Thomas Young Centre, Imperial College London, South Kensington, London SW7 2AZ, UK

<sup>2</sup> Departamento de Física and CICECO, Universidade de Aveiro, 3810-193 Aveiro, Portugal

<sup>3</sup> IFIMUP and IN-Institute of Nanoscience and Nanotechnology, 4169-007 Porto, Portugal

<sup>4</sup> CRANN and School of Physics, Trinity College Dublin—Dublin 2, Ireland

E-mail: [romi.korotana09@alumni.imperial.ac.uk](mailto:romi.korotana09@alumni.imperial.ac.uk)

Received 6 March 2016, revised 14 May 2016

Accepted for publication 24 May 2016

Published 21 June 2016



## Abstract

Manganites with the formula  $\text{La}_{1-x}\text{Ca}_x\text{MnO}_3$  for  $0.2 < x < 0.5$  undergo a magnetic field driven transition from a paramagnetic to ferromagnetic state, which is accompanied by changes in the lattice and electronic structure. An isotropic expansion of the  $\text{La}_{0.75}\text{Ca}_{0.25}\text{MnO}_3$  cell at the phase transition has been observed experimentally. It is expected that there will be a large entropy change at the transition due to its first order nature. Doped lanthanum manganite (LMO) is therefore of interest as the active component in a magnetocaloric cooling device. However, the maximum obtained value for the entropy change in Ca-doped manganites merely reaches a moderate value in the field of a permanent magnet. The present theoretical work aims to shed light on this discrepancy. A combination of finite temperature statistical mechanics and first principles theory is applied to determine individual contributions to the total entropy change of the system by treating the electronic, lattice and magnetic components independently. Hybrid-exchange density functional (B3LYP) calculations and Monte Carlo simulations are performed for  $\text{La}_{0.75}\text{Ca}_{0.25}\text{MnO}_3$ . Through the analysis of individual entropy contributions, it is found that the electronic and lattice entropy changes oppose the magnetic entropy change. The results highlighted in the present work demonstrate how the electronic and vibrational entropy contributions can have a deleterious effect on the total entropy change and thus the potential cooling power of doped LMO in a magnetocaloric device.

Keywords: manganites, DFT, oxides, phase transitions, entropy, Monte Carlo simulations, magnetocalorics

(Some figures may appear in colour only in the online journal)

## 1. Introduction

The magnetocaloric effect (MCE) [1–5] is defined as the change in temperature of a magnetically ordered material, upon the application or removal of an external magnetic field

under adiabatic conditions. The effect was first discovered by Weiss and Piccard, in 1917, when a sizable and reversible temperature change was observed in Nickel near its Curie temperature [6, 7]. In the past two decades, there has been a surge of interest in magnetocaloric materials that could

potentially be used in cooling devices, such as heat pumps and magnetic refrigerators [8–11]. More recently, manganites, an economically viable class of materials, have attracted much attention due to their remarkable structural and electronic properties, which are strongly dependent on the doping concentration as well as external variables, such as temperature, pressure, and electric or magnetic fields [4].

Manganites have the general formula  $R_{1-x}A_xMnO_3$ , where R is a trivalent rare earth metal and A is a divalent alkaline earth element. Perovskites-type manganites exhibit cross-coupling between the spin, charge, orbital and lattice degrees of freedoms [12–14]. This strong interplay often leads to non-trivial material responses to external stimuli. However, due to the effects of strong electron correlation, a complete microscopic understanding of the physics underlying the properties of manganites has not yet been obtained.

Since the discovery of the Colossal magnetoresistance (CMR) [15–17], experimental studies on manganites doped with divalent alkaline earth elements, such as Ca, Ba and Sr, have been the subject of intense study. An important practical feature of manganites is that the average radii of cations at different sites can affect the lattice and electronic structure [2]. The crystal structure, in particular, accommodates a wide variety of dopants at the A-site without undergoing a phase transition. Furthermore, doping at the R-site is of interest since the exchange interaction could be modified via the magnetic cation. This provides a mechanism for tuning the MCE and the Curie temperature  $T_C$  i.e. the operating temperature of the cooling device.

The  $La_{1-x}Ca_xMnO_3$  series for  $0.2 < x < 0.5$  undergoes a field driven transition from a paramagnetic insulating (PM-I) to ferromagnetic metallic (FM-M) state, which is accompanied by changes in the lattice and electronic structure. As determined by Radaelli *et al.*, from high-resolution synchrotron X-ray powder diffraction data, an isotropic expansion of the  $La_{0.75}Ca_{0.25}MnO_3$  cell occurs at the transition without affecting the orthorhombic symmetry [18]. It is therefore expected that the isothermal entropy change  $\Delta S_{iso}$  for this particular composition would be considerable, since the electronic and lattice contributions may play a significant role in enhancing the MCE in addition to the expected contribution from spin disorder [18, 19]. Despite many experimental efforts to enhance the  $\Delta S_{iso}$  in  $La_{1-x}Ca_xMnO_3$  manganites, particularly for  $0.2 < x < 0.5$ , the MCE reaches a modest value in the field of a permanent magnet [4, 16, 20–28]. The maximum obtained value for  $La_{0.75}Ca_{0.25}MnO_3$  is  $-4.70 \text{ J kg}^{-1} \text{ K}^{-1}$  [20] for an applied external magnetic field of 1.5 T. However, materials which experience a magnetostructural phase transition such as the  $Gd_5(Si,Ge)_4$  family exhibit a relatively larger MCE. For example, the MCE determined experimentally for  $Gd_5(Si_{0.5}Ge_{0.5})_4$  for an applied magnetic field of 2 T is  $-14 \text{ J kg}^{-1} \text{ K}^{-1}$  [8].

A predictive, microscopic theory of the MCE requires a calculation of the Gibbs free energy change at the transition which can be expressed as [29]:

$$G(T, P, H) = U_{vib} + U_{elas} + U_{elec} + U_{ex} - MH + PV - TS \quad (1)$$

where the first four terms correspond to the internal energy (vibrational, elastic, electronic and magnetic, respectively). In the current study we make the fundamental assumption that the entropy change can be expressed as,

$$\Delta S_{total} = \Delta S_{vib} + \Delta S_{elas} + \Delta S_{elec} + \Delta S_{mag} \quad (2)$$

where  $\Delta S_{vib}$ ,  $\Delta S_{elas}$ ,  $\Delta S_{elec}$  and  $\Delta S_{mag}$  are the vibrational, elastic, electronic and magnetic contributions, respectively. Equation (2) corresponds to the isothermal entropy change  $\Delta S_{iso}$  when a magnetic field is applied, which can also be determined through integration of the thermodynamic Maxwell relation. This assumption neglects the explicit interactions between lattice, spin and electronic degrees of freedom. We test the assumption of independent contributions for a simple periodic model.

The paper is organized as follows: in section 2 the computational methodology is provided and the results are presented in section 3. The discussion begins with the electronic entropy calculation for  $La_{0.75}Ca_{0.25}MnO_3$ , followed by an analysis of the lattice component, which includes both the elastic and vibrational contributions. The discussion then focuses on a Monte Carlo study of the magnetic entropy and magnetization dynamics of the doped manganite composition. Conclusions are drawn in section 4.

## 2. Methodology

All calculations have been performed using CRYSTAL09 [30] which is based on the expansion of the crystalline orbitals as a linear combination of a local basis set (BS) consisting of atom centered Gaussian orbitals.

The Mn, O and Ca ions are described by a triple valence all-electron BS: an 86-411d(41) contraction (one *s*, four *sp*, and two *d* shells), an 8-411d(1) contraction (one *s*, three *sp*, and one *d* shells) and an 8-65111(21) contraction (one *s*, three *sp*, and two *d* shells), respectively; the most diffuse *sp(d)* exponents are  $\alpha^{Mn} = 0.4986(0.249)$ ,  $\alpha^O = 0.1843(0.6)$  and  $\alpha^{Ca} = 0.295(0.2891) \text{ Bohr}^{-2}$ . The La basis set includes a relativistic pseudopotential to describe the core electrons, while the valence part consists of a 411p(411)d(311) contraction scheme (with three *s*, three *p* and three *d* shells); the most diffuse exponent is  $\alpha^{La} = 0.15 \text{ Bohr}^{-2}$  for each *s*, *p* and *d* [31].

Electron exchange and correlation are approximated using the B3LYP hybrid exchange functional, which is expected to be more reliable than LDA or GGA approaches for transition metal oxides [32–35]. The exchange and correlation potentials and energy functional are integrated numerically on an atom centered grid of points. The integration over radial and angular coordinates is performed using Gauss–Legendre and Lebedev schemes, respectively. A pruned grid consisting of 99 radial points and 5 sub-intervals with (146, 302, 590, 1454, 590) angular points has been used for all calculations (the XXLGRID option implemented in CRYSTAL09 [30]). This grid converges the integrated charge density to an accuracy of about  $\times 10^{-6}$  electrons per unit cell. The Coulomb and exchange series are summed directly and truncated using overlap criteria with thresholds of  $10^{-7}$ ,  $10^{-7}$ ,  $10^{-7}$ ,  $10^{-7}$

**Table 1.** The electronic entropy contribution  $\Delta S_{\text{elec}}$  to  $\Delta S$  for the FM-M ( $\text{La}_{0.75}\text{Ca}_{0.25}\text{MnO}_3$ ) at 10 K, 100 K and 224 K ( $T_C = 224$  K [20, 40]), where  $S_{\text{elec}}$  for the FM-I is considered to be zero.

Temperature (K)	$\Delta S_{\text{elec}}$ (J mol <sup>-1</sup> K <sup>-1</sup> )
10	0.01
100	0.19
224	0.45

and  $10^{-14}$  as described previously [30, 36]. Reciprocal space sampling was performed on a Pack–Monkhorst net with a shrinking factor  $IS = 8$ , which defines 75 symmetry unique  $k$ -points in the Brillouin zone of the primitive cell. The self consistent field procedure was converged to a tolerance in the total energy of  $\Delta E = 1 \cdot 10^{-7} E_h$  per unit cell.

The cell parameters and the internal coordinates have been determined by minimization of the total energy within an iterative procedure based on the total energy gradient calculated analytically with respect to the cell parameters and nuclear coordinates. Convergence was determined from the root-mean-square (rms) and the absolute value of the largest component of the forces. The thresholds for the maximum and the rms forces (the maximum and the rms atomic displacements) have been set to 0.000 45 and 0.000 30 (0.001 80 and 0.0012) in atomic units. Geometry optimization was terminated when all four conditions were satisfied simultaneously.

The FM-PM phase transition has been investigated by mapping the first principles energies to the 3D Ising model in a Monte Carlo approach. A simple cubic lattice with periodic boundary conditions is considered and it is assumed that interactions occur only between nearest neighbouring spin states. The Ising Hamiltonian,  $\hat{H}^{\text{mag}}$  is defined as:

$$\hat{H}^{\text{mag}} = -\frac{1}{2} \sum_{\langle i,j \rangle} J_{ij} S_i^z S_j^z - \sum_i H_{\text{ext}} S_i^z \quad (3)$$

where  $H_{\text{ext}}$  is an external magnetic field,  $J_{ij}$  is the exchange parameter and  $S$  is the spin state, which can only take on the value  $-1$  (spin *down*) or  $1$  (spin *up*). In the Ising model, only the  $z$  component of the spin variable is considered.

Here the relevant thermodynamic parameters such as the magnetization dependence on temperature and applied magnetic field, and corresponding MCE near  $T_C$  are numerically estimated via the random path sampling (RPS) Monte Carlo method for  $\text{La}_{0.75}\text{Ca}_{0.25}\text{MnO}_3$  [37]. The RPS method allows a flat magnetization sampling histogram of magnetic configurations, by construction. Energy and magnetization sampling is performed via local updates from  $+1$  and  $-1$  total magnetization states. Prior to each sweep, a shuffled list of spin positions is generated. Spin flips, where a spin in the  $+1$  state is flipped with the probability of 1, are then performed sequentially using this list. The configuration energy is determined via the local energy difference due to a spin flip, as usually done in the Metropolis algorithm. From the obtained joint density of states (JDos), the partition function is evaluated for each desired  $(H, T)$  value and therefore, the corresponding thermodynamic variables and their  $(H, T)$  dependence. This approach compares favourably to the use of the Metropolis algorithm in

**Table 2.** The vibrational entropy for  $\text{La}_{0.75}\text{Ca}_{0.25}\text{MnO}_3$ , in the FM-M and FM-I states for the supercell.

M/I	$S_{\text{vib}}$ (J mol <sup>-1</sup> K <sup>-1</sup> )
M	92.97
I	88.33
$\Delta S_{\text{vib}}$	<i>4.64</i>

Note: The  $\Delta S_{\text{vib}}$  is given in italics in units of J mol<sup>-1</sup> K<sup>-1</sup>.

the context of MCE studies, as critical slowing down effects near  $T_C$  are avoided, and individual  $(H, T)$ -dependent calculations are unnecessary, as the more time-consuming JDos evaluation is independent of these extensive parameters.

### 3. Results

#### 3.1. Electronic entropy

The magnetic phase transition in  $\text{La}_{0.75}\text{Ca}_{0.25}\text{MnO}_3$  is accompanied by a metal–insulator (M–I) transition which results in a modification of the density of states at the Fermi level, and strong evidence for this has been provided in a recent theoretical study [38]. Thus, the electronic entropy for the M and I phases is expected to differ significantly. The electronic structure determined for the M and I, from hybrid density functional theory calculations [38], is used to compute the  $\Delta S_{\text{elec}}$  for  $\text{La}_{0.75}\text{Ca}_{0.25}\text{MnO}_3$ . This contribution is computed using the finite temperature DFT approach [39], which allows one to express the free energy in terms of the Fermi function,

$$f_{ik} = (1 + e^{\frac{(\epsilon_{ik} - \epsilon_F)}{k_B T}})^{-1}, \quad (4)$$

$$S_{\text{electronic}} = 2 \sum_{i,k}^{N_{\text{states}}} (f_{ik} \ln f_{ik} + (1 - f_{ik}) \ln(1 - f_{ik})) k_{i,\text{weight}}, \quad (5)$$

where  $N$  is the number of (occupied and unoccupied) states,  $f_{ik}$  is the Fermi distribution function and  $k_{i,\text{weight}}$  is the  $k_i$  point geometrical integration weight, respectively. The Fermi function describes the probability of occupation at a certain temperature, which can be summed over all the  $k$ -points in the Brillouin zone for each band to determine the occupation levels.

The computed values of the electronic entropy,  $\Delta S_{\text{elec}}$  at 10 K, 100 K and 224 K ( $T_C$ ) are given in table 1. The values are positive, since  $S_{\text{elec}}$  for the insulator is zero and the field-driven transition is from an I to a M. Thus, as the temperature is increased from 10 K to 224 K, the  $\Delta S_{\text{elec}}$  increases.

#### 3.2. Lattice entropy

**3.2.1. Elastic contribution.** The elastic contribution  $\Delta S_{\text{elas}}$  to the total entropy change is based on the deformation of the crystal structure. According to Hooke’s law, and assuming that the bulk modulus is constant, the elastic entropy change is given by the following [29]:

$$\Delta S_{\text{elas}} = \frac{1}{T_C} \frac{B}{2} \left( \frac{\Delta V}{V_0} \right)^2 \quad (6)$$

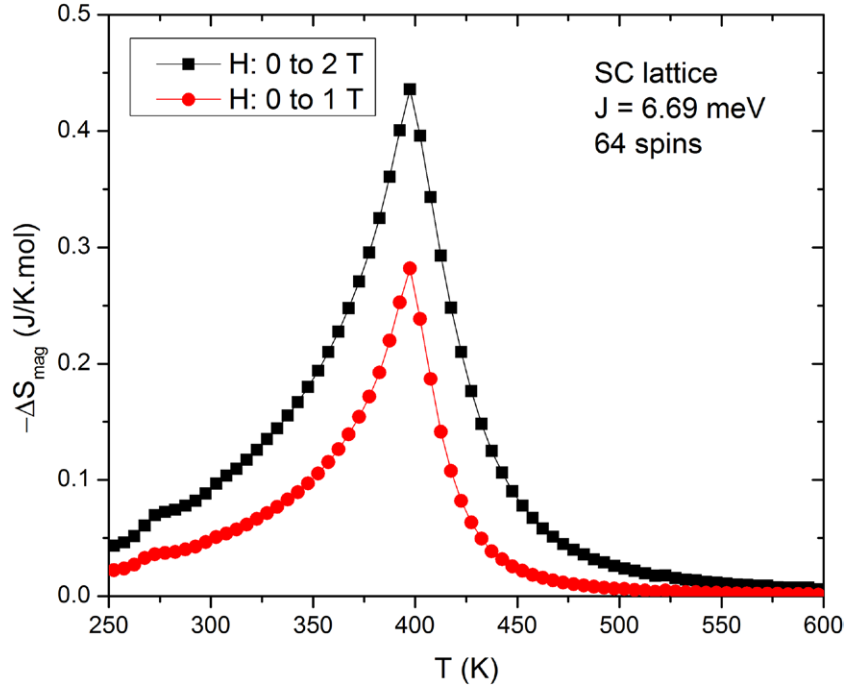


**Figure 1.** The magnetic entropy change  $\Delta S_{\text{mag}}$  due to an applied magnetic field of 1 and 2 T as a function of temperature calculated for  $J = 6.69$  meV.

where  $V_0$  is the initial volume. The value for the bulk elastic modulus  $B$  is taken to be 100 GPa, which has been determined from the ultrasonic properties of  $\text{La}_{0.67}\text{Ca}_{0.33}\text{MnO}_3$  [41]. The  $\Delta V$  in this particular calculation corresponds to the difference in volume between the FM-M ( $244.8 \text{ \AA}^3$ ) and FM-I ( $245.1 \text{ \AA}^3$ ) state from the DFT calculations, which is  $0.3 \text{ \AA}^3$  [38]. If the experimental  $T_C$  of 224 K [20] is assumed, the  $\Delta S_{\text{elas}}$  is  $1.81 \times 10^{-4} \text{ J mol}^{-1} \text{ K}^{-1}$ . The elastic contribution to  $\Delta S$  may therefore be considered to be negligible. If, however, we assume the  $\Delta V/V \approx 0.13\%$  determined from high-resolution synchrotron X-ray powder diffraction data [18], then the  $\Delta S_{\text{elas}}$  is estimated to be  $2.03 \times 10^{-4} \text{ J mol}^{-1} \text{ K}^{-1}$ . Thus, the experimental and theoretical estimates for  $\Delta S_{\text{elas}}$  agree rather well but both are essentially negligibly small.

**3.2.2. Vibrational contribution.** The vibrational entropy of the two phases can differ due to the significant change in the electronic structure and bonding. This change can be estimated by computing the vibrational entropy in the quasi-harmonic approximation which requires a sampling of the vibrational modes. In order to sample the vibrational modes, the vibrational frequencies for an isotropic (80 atom) supercell are computed to determine the vibrational contribution  $S_{\text{vib}}$  to  $\Delta S$ . The mass-weighted Hessian (or dynamical) matrix [42] is calculated by numerical evaluation of the first derivative of the analytical atomic gradients; and diagonalised to obtain the phonon frequencies at the Gamma point of the supercell. The vibrational entropy  $S_{\text{vib}}$  has been calculated using the following,

$$F_{\text{vib}} = E_0 + \frac{1}{2} \sum_{k,j} \hbar \omega + k_B T \sum_{k,j} \ln [1 - \exp(-\hbar \omega / k_B T)] \quad (7)$$

$$S_{\text{vib}} = - \frac{\partial F_{\text{vib}}}{\partial T}. \quad (8)$$

The  $S_{\text{vib}}$  for the metallic and insulating state is given in table 2.

The  $S_{\text{vib}}$  for the metal is higher than that of the insulator which is attributed to phonon mode softening in the metallic state. Therefore, the contribution of  $\Delta S_{\text{vib}}$  is also positive.

### 3.3. Magnetic entropy

The Ising Hamiltonian has been parameterised with the exchange coupling constant of 6.69 meV calculated by averaging the apical ( $J_{\text{ap}}$ ) and equatorial ( $J_{\text{eq}}$ ) determined from hybrid-exchange DFT calculations for the FM-M state [38]. The  $\text{Mn}^{3.75+}$  is described by a classical Ising spin, and the La, Ca and O ions are considered to be non-magnetic in the MC simulations. The number of sites used in the simulation of a simple cubic (SC) lattice is 64, and the magnetization values were obtained by finding the minimum of the free energy evaluated from the partition function at the desired  $(H, T)$  values. The number of RPS sweeps performed was  $10^{11}$ , leading to a free energy convergence better than 0.001% for  $T$  near  $T_C$ , under zero applied field. The magnetic entropy has then been computed as:

$$\Delta S_{\text{mag}}(T, \Delta H) = \int_{H_0}^H \left( \frac{\partial M(T, H)}{\partial T} \right) dH. \quad (9)$$

The field-induced magnetic entropy change  $\Delta S_{\text{mag}}$  has been computed for  $\Delta H$  of 1 and 2 T and is shown in figure 1.

The predicted  $T_C$  of  $\sim 398$  K has been determined from the peak in the  $\Delta S_{\text{mag}}$  curve. This  $T_C$  value is larger than the experimental values of  $\sim 240$  K for the bulk



$\text{La}_{0.75}\text{Ca}_{0.25}\text{MnO}_3$  compound [40], and also 177 K and 224 K for  $\text{La}_{0.75}\text{Ca}_{0.25}\text{MnO}_3$  nanoparticles with average sizes of 120 and 300 nm, respectively [20]. The overestimation of  $T_C$  determined here may result from the simplified magnetic model employed; particularly since the average isotropic interaction of only nearest neighbors is considered. A sizable contribution to the isothermal entropy is also neglected since a rigid lattice with no magnetovolume coupling interaction is implemented.

The maxima of the field-induced  $\Delta S_{\text{mag}}$  occurs in the vicinity of  $T_C$  and the determined values for  $\Delta H$  of 1 and 2 T are  $-0.284$  and  $-0.438 \text{ J mol}^{-1} \text{ K}^{-1}$ , respectively. The computed values are significantly smaller than the experimental  $\Delta S_{\text{iso}}$  determined from magnetization measurements (defined as the maximum slope in  $dM/dT$ ) of  $\text{La}_{0.75}\text{Ca}_{0.25}\text{MnO}_3$  for an applied magnetic field of 1.5 T [20]. Furthermore, through the computation of  $\Delta S_{\text{mag}}$  for the experimental  $T_C$  (not shown), which is implicitly varied through the exchange coupling constant in the Monte Carlo simulations, the value is  $\sim 15\%$  larger but is also comparatively small when compared to experiment.

#### 4. Conclusions

A combined hybrid-exchange DFT and Monte Carlo approach has been used to quantify the electronic, lattice and magnetic entropy contributions, to the entropy change  $\Delta S$  across the PM-I to FM-M transition, in  $\text{La}_{0.75}\text{Ca}_{0.25}\text{MnO}_3$ . It has been predicted that the electronic and magnetic contributions are of a similar magnitude. Further, the computed electronic and lattice entropy terms oppose the magnetic one. Thus, the electronic and vibrational terms have a destructive effect on the total entropy change. The formalism adopted herein has provided a valuable insight into the competing entropy components for  $\text{La}_{0.75}\text{Ca}_{0.25}\text{MnO}_3$ . The effects of more complex interactions such as spin–lattice and spin–orbit on the entropy change should be considered. However, MC simulations of a magnetovolume coupled Ising hamiltonian would require a study of the  $J$  value dependence on lattice volume which is intractable at the current time. The microscopic optimization of such interactions, to enhance the magnetocaloric properties, may become a valuable tool in the search for new magnetocaloric materials.

#### Acknowledgments

We thank L F Cohen, K G Sandeman and J A Turcaud of The Blackett Laboratory, Imperial College London for useful discussions. The EPSRC Grant (EP/G060940/1) on Nanostructured Functional Materials for Energy Efficient Refrigeration, Energy Harvesting and Production of Hydrogen from Water is gratefully acknowledged. This work made use of the high performance computing facilities of Imperial College London and-via membership of the UK's HPC Materials Chemistry Consortium funded by EPSRC (EP/L000202)-of ARCHER, the UK's national high-performance computing service, which is provided by UoE HPCx Ltd. at the University of Edinburgh, Cray Inc. and NAG Ltd., and funded by the Office of Science and Technology through

EPSRC. This work was developed within the scope of the project CICECO-Aveiro Institute of Materials, POCI-01-0145-FEDER-007679 (FCT Ref. UID/CTM/50011/2013), financed by national funds through the FCT/MEC and when appropriate co-financed by FEDER under the PT2020 Partnership Agreement. JSA acknowledges FCT SFRH/BPD/111270/2015 grant. ZG acknowledges the financial support from a Marie Curie Intra European Fellowship within the 7th European Community Framework Programme.

#### References

- [1] Gómez J R, Garcia R F, Catoira A D M and Gómez M R 2013 *Renew. Sustain. Energy Rev.* **17** 74
- [2] Franco V, Blázquez J, Ingale B and Conde A 2012 *Annu. Rev. Mater. Res.* **42** 305
- [3] Sandeman K G 2012 *Scr. Mater.* **67** 566
- [4] Phan M and Yu S 2007 *J. Magn. Magn. Mater.* **308** 325
- [5] Pecharsky V K and Gschneidner K A 2006 *Int. J. Refrig.* **29** 1239
- [6] Weiss P and Piccard A 1917 *J. Phys. Theor. Appl.* **7** 103
- [7] Smith A 2013 *Eur. Phys. J. H* **38** 507
- [8] Pecharsky V K and Gschneidner K A 1997 *Phys. Rev. Lett.* **78** 4494
- [9] Yu B F, Liu M and Egolf P W 2010 *Int. J. Refrig.* **33** 1029–60
- [10] Rowe A 2011 *Int. J. Refrig.* **34** 168
- [11] Neilsen K K, Tusek J, Engelbrecht K, Schopfer S and Schopfer A 2011 *Int. J. Refrig.* **34** 603
- [12] Rao C N R and Raveau B 1998 *Colossal Magnetoresistance, Charge Ordering and Related Properties of Managase Oxides* (Singapore: World Scientific)
- [13] Dagotto E, Hotta T and Moreo A 2001 *Phys. Rep.* **344** 1
- [14] Tokura Y 1999 *Colossal Magnetoresistance Oxides* (London: Gordon and Breach)
- [15] Jonker G H and Santen J H 1950 *Physica* **16** 337
- [16] Morelli A J, Mance A M, Mantese J V and Micheli A L 1996 *J. Appl. Phys.* **79** 373
- [17] Salamon M B and Jaime M 2001 *Rev. Mod. Phys.* **73** 583
- [18] Radaelli P G, Cox D E, Marezio M, Cheong S-W, Schiffer P E and Ramirez A P 1995 *Phys. Rev. Lett.* **75** 4488
- [19] Kim K H, Gu J Y, Choi H S, Park G W and Noh T W 1996 *Phys. Rev. Lett.* **77** 1877
- [20] Guo Z B, Zhang J R, Huang H, Ding W P and Du Y W 1997 *Appl. Phys. Lett.* **70** 904
- [21] Phan M H, Pham V T, Yu S and Rhee J R 2004 *J. Magn. Magn. Mater.* **272–6** 2337
- [22] Phan M H, Yu S, Hur N H and Yeong Y H 2004 *J. Appl. Phys.* **96** 1154
- [23] Phan M H, Tian S B, Yu S and Hur N H 2003 *Physica B* **327** 211
- [24] Xu Q Y, Gu K M, Liang X L, Ni G, Wang Z M, Sang H and Du Y W 2001 *J. Appl. Phys.* **90** 524
- [25] Zhang X X, Tejada J, Xin Y, Sun G F, Wong K W and Bohigas X 1996 *Appl. Phys. Lett.* **69** 3596
- [26] Hueso L E, Sande P, Miguens D R, Rivas J, Rivadulla F and Lopez-Quintela M A 2002 *J. Appl. Phys.* **91** 9943
- [27] Sun Y, Xu X and Zhang Y H 2000 *J. Magn. Magn. Mater.* **219** 183
- [28] Bohigas X, Tejada J, Martinez-Sarrion M L, Tripp S and Black R 2000 *J. Magn. Magn. Mater.* **208** 85
- [29] Jia L, Liu G J, Sun J R, Zhang H W, Hu F X, Dong C, Rao G H and Shen B G 2006 *J. Appl. Phys.* **100** 123904
- [30] Dovesi R et al 2009 *CRYSTAL09 User's Manual* (Torino: University of Torino)
- [31] Muñoz D, Harrison N M and Illas F 2004 *Phys. Rev. B* **69** 085115
- [32] Muscat J and Harrison N M 2001 *Chem. Phys. Lett.* **342** 2016

- [33] Cora F, Alfredsson M, Mallia G, Middlemiss D S, Mackrodt W C, Dovesi R and Orlando R 2004 *The Performance of Hybrid Density Functionals in Solid State Chemistry* vol 113 (Berlin: Springer)
- [34] Adamo C, Ernzerhof M and Scuseria G E 2000 *J. Chem. Phys.* **112** 2643
- [35] Kurth S, Perdew J P and Blaha P 1999 *Int. J. Quantum Chem.* **75** 889
- [36] Pisani C, Dovesi R and Roetti C 1988 *Hartree-Fock Ab Initio Treatment of Crystalline Systems (Lecture Notes in Chemistry* vol 48) (Heidelberg: Springer)
- [37] Amaral J S, Goncalves J N and Amaral V S 2014 *IEEE Trans. Magn.* **50** 1002204
- [38] Korotana R, Mallia G, Gercsi Z, Liborio L and Harrison N M 2014 *Phys. Rev. B* **89** 205110
- [39] Mermin N D 1965 *Phys. Rev.* **137** 1441
- [40] Schiffer P, Ramirez A P, Bao W and Cheong S-W 1995 *Phys. Rev. Lett.* **75** 3336
- [41] Zhu C, Zheng R, Su J and He J 1999 *Appl. Phys. Lett.* **74** 3504
- [42] Pascale F, Zicovich-Wilson C M, Gejo F L, Civalleri B, Orlando R and Dovesi R 2004 *J. Comput. Chem.* **25** 888